HHS Public Access

Taking Paclitaxel Coated Balloons to a Higher Level: predicting coating dissolution kinetics, tissue retention and dosing dynamics

Abraham R. Tzafriri[1,*], **Sahil A. Parikh**[2], **Elazer R. Edelman**[3]

[1]CBSET Inc., Lexington, MA

[2]New York Presbyterian Hospital/Columbia University Irving Medical Center and Columbia University Vagelos College of Physicians and Surgeons, New York, NY

[3]Institute for Medical Engineering and Science, MIT, Cambridge, MA and Cardiovascular Division, Brigham and Women's Hospital, Harvard Medical School, Boston, MA

Abstract

Paclitaxel coated balloons (PCBs) are a promising non-implantable alternative to drug-eluting stents, whereby drug is delivered to the arterial wall in solid form as a semi-continuous solid coating or as micro drug depots. To date, it has been impossible to predict or even infer local tissue dosing levels and persistence, making it difficult to compare *in vivo* performance of different devices in healthy animals or to extrapolate such data to diseased human arteries. Here we derive and analyze a coupled reaction diffusion model that accounts for coating dissolution and tissue distribution, and predicts the concentration of dissolved drug in the tissue during and post dissolution.

Time scale analysis and numerical simulations based on estimated diffusion coefficients in healthy animal and diseased human arteries both imply that dissolution of crystalline paclitaxel coating is mass transfer coefficient-limited, and can therefore be solved for independently of the tissue transport equations. Specifically, coating retention is predicted to follow piecewise linear kinetics, reflecting the differential and faster dissolution of lumenal versus tissue-embedded coating owing to a disparity in convective forces. This prediction is consistent with published data on a range of PCBs and allowed for the estimation of the associated dissolution rate-constants and the maximal soluble drug concentration in the tissue during coating dissolution. Maximal soluble drug concentration in the tissue scales as the product of the solubility and ratio of the dissolution and diffusion rate-constants. Thus, coatings characterized by micromolar solubilities give rise to nanomolar soluble concentrations in healthy animal arteries and ~0.1 micromolar in calcified atherosclerotic arteries owing to slower tissue diffusion. During dissolution, retention in porcine iliofemoral arteries is predicted to be dominated by solid coating, whereas post dissolution it is dominated by receptor-bound drug (3.7 ng receptors/g tissue).

*Corresponding author at: 500 Shire Way, Lexington, MA – 02421. rtzafriri@cbset.org.

Paclitaxel coating dissolution and dosing kinetics can now be modeled based upon accepted principles of surface dissolution and tissue transport to provide insights into the dependence of clinical efficacy on device properties and the interplay of lesion complexity and procedural parameters.

Keywords

Binding; Diffusion; Drug coated balloons; Retention; Toxicity

1. Introduction

Paclitaxel coated balloons have been developed as an alternative to drug-eluting stents, and have seen particular success in the treatment of peripheral artery disease[1]. The efficacious delivery of paclitaxel from balloons has been attributed to several factors, including the drug's high lipophilicity which contributes to high tissue retention and intracellular penetration, potent inhibition of smooth muscle cell migration and proliferation[2, 3], and additives and excipients which can optimize coating adherence, release and transfer to the vessel wall[4].

The type of additive used and the formulation method also affect the morphology of the coating and its solubility, and with it tissue retention[5]. The range of possible morphologies is high, as paclitaxel is known to be polymorphous, existing as one of three primary forms under ambient conditions[6], amorphous solid, anhydrous crystals, or dihydrate crystals, with the crystalline forms exhibiting 1–2 orders of magnitude lower aqueous solubilities compared to the amorphous form[6, 7]. All three forms have been coated onto balloons and metallic stents, in pure (Figure 1A) or mixed form (Figure 1B). Thus for example, Granada et al reported the use of balloons coated with purely amorphous or purely dihydrate paclitaxel[8], the Zilver PTX® stent employs a mixed amorphous-dihydrate paclitaxel coating[9], and patents have been submitted for balloons coated with anhydrous paclitaxel in combination with other paclitaxel polymorphs[10–12].

Despite the wide adoption of PCB, many questions remain as to their mode of action, efficacy and safety. Though first evaluated for treatment of coronary artery disease with some early promise, adoption has been slow and focused on complex lesion subsets where stents are suboptimal, e.g. in-stent restenosis, bifurcation lesions, diffuse lesions and small vessels where stents are suboptimal. Thus, over the years, focus has shifted to the treatment of peripheral artery disease using PCB, with impressive results in femoropopliteal arteries but limited efficacy in infrapopliteal arteries. The success of PCB in some vascular beds but not in others remains an enigma. Moreover, a recent meta-analysis of randomized controlled trials investigating paclitaxel-coated balloons and stents in the femoral and/or popliteal arteries reported an increased risk of death at 2 and 5 years post treatment compared to devices not coated with paclitaxel[13]. While some have questioned the validity of this clinical meta-analysis on the basis of its assumptions and more recent clinical data[14, 15], there is currently no theoretical framework for these devices that could predict the duration of coating retention and tissue dosing based on coating parameters and tissue properties.

Based on the experience with drug-eluting stents, the tissue-retained dose and its residence time are believed to determine biological effects and explain the lack of a class effect for these devices[16]. Yet, whereas traditional polymer-coated stents elute drug in a soluble and pharmacologically active form, balloon delivered coatings are pharmacologically inert, serving as local depots for release of pharmacologically active drug. Thus, comparisons of PCB with different coating morphologies on the basis of loading or even measured tissue retention are unfounded, as given the inertness of solid drug, both measurable quantities are not generally indicative of the pharmacologically active drug pool in the tissue[17]. What is needed is the development of methods for discriminating between the time course of soluble free and tissue-bound drug and residual solid coating on and within the tissue. Here we achieve these goals using computational modeling. Specifically, we derive and analyze a coupled reaction diffusion model that accounts for coating dissolution and tissue distribution for clinically relevant devices and predicts the kinetics of tissue-delivered drug including relative dissolution rates and residual amounts of lumenal and tissue embedded coating, as well as the concentration of dissolved drug in the tissue during and post dissolution. Local drug effects in the artery wall are predicted based on receptor occupancy and the scaling of extracellular soluble drug concentrations relative to the picomolar threshold concentrations for inhibition of human cell proliferation [18] and migration[19] in cell culture (IC50). Extracellular soluble drug concentration and receptor occupancy both predict persistence of biological effects for several months in healthy animal arteries and up to 3 years in calcified human arteries, though at concentrations deemed unlikely to exert off-target toxicities.

2. Modeling Methods

Balloon inflation applies the balloon coating against the artery where it either remains on the mural interface or lodges into deeper tissue layers in particulate form[4, 24] (Figure 2A). The amount of coating in each of these compartments depends on many factors including those related to the lesion, e.g. morphology, integrity, irregularities, and balloon properties like coating morphology, balloon inflation pressure and duration, balloon and tissue compliance, and drug particle size. Similarly, the mural-adherent coating may be transferred as large or small patches across the entire or part of the treated length. Either way, drug coating dissolution occurs via diffusion across a stagnant boundary layer of already dissolved drug (Figure 2B).

Consequently, the flux of dissolving drug into the surrounding environment is governed by the product of the concentration gradient across the boundary layer, C_s-C, and a mass transfer coefficient k_c,

$$\text{dissolution flux} = k_c(C_s - C). \quad [1]$$

Here C_s is the interstitial solubility of the drug. Importantly, local transport near the dissolving particle will affect both the concentration of soluble drug at the boundary edge and the mass transfer coefficient k_c owing to the dependence the boundary layer thickness on ambient flow[25]. Consequently, Eq. 1 is analyzed separately below depending on whether the dissolving coating surface is blood or tissue contacting.

2.1   Dissolution into blood

Owing to the efficiency of mixing by pulsating blood and its capacity to absorb drug, the concentration of soluble drug in the vessel lumen is expected to be much lower than that in the tissue. Indeed, the reported early peak plasma concentrations post PCB and Zilver PTX of 0.8–54 ng/mL[20, 22, 26, 27] are 6-fold lower than the lowest reported aqueous solubility of paclitaxel[6, 7] (300 ng/mL). Moreover, paclitaxel solubility in plasma is increased 20–60 fold due to its extensive binding to plasma proteins[28, 29]. Consequently, in evaluating the lumenal dissolution flux into blood we can neglect the concentration of soluble drug in Eq. 1 to obtain

$$\text{lumenal dissolution flux} \approx k_c^L C_s. \quad [1L]$$

The superscript L was added to denote the lumenal value of the mass transfer rate-constant. By the same token, lumenal dissolution does not contribute to tissue dosing.

2.2   Mass transfer coefficient limited dissolution and tissue dosing

The tissue contacting side of the adherent coating and any tissue embedded coating particles dissolve under non-sink conditions as the forces of extracellular convection and diffusion are orders of magnitude slower than lumenal convection. Moreover, for low molecular-weight drugs such as paclitaxel, transmural convective transport can be neglected relative to diffusion[30]. As the dissolution flux is equal to the local diffusive flux, its magnitude is determined by the coupled forces of extracellular diffusion, cell uptake and binding in both compartments (Figure 3). The equations describing tissue level transport are provided the online Supplement along with relevant parameter estimates and numerical methods for the solution of these reaction-diffusion equations[31, 32]. However, as we proceed to argue, the rate of paclitaxel coating dissolution is mass transfer coefficient limited, which allows for an analytical pseudo-steady state approximation of the diffusive flux and the concentration of soluble drug at the coating-tissue interface[33].

Indeed, whereas clinically relevant paclitaxel coatings are designed to dissolve over the course of days to weeks, owing to its small size paclitaxel quickly diffuses through peripheral animal arteries with rate-constants $k_{tiss} = D/L^2$ on the order 1.4–7.3 h^{-1} [34–36] where D is the tissue diffusivity and L is the wall thickness. Consequently, in evaluating the lumenal dissolution flux into the tissue we can safely neglect the concentration of soluble drug in Eq. 1 to obtain

$$\text{tissue dissolution flux} \approx k_c^T C_s, \quad [1T]$$

Moreover, as mass transfer is rate limiting, the transmural distribution of soluble extracellular drug will be well approximated by its pseudo-steady state linear distribution, and the diffusive flux at the dissolving coating surfaces can be estimated as $-(D/L) C_{max}$ where C_{max} is the soluble drug concentration at the tissue interface of the stagnant boundary layer, and due to tissue diffusion also the maximal soluble drug concentration in the tissue.

Flux continuity at the coating-tissue interface dictates that sum of dissolution flux and the diffusion flux is zero

$$k_c^T C_s - (D/L)C_{max} = 0.$$

Isolating C_{max} we arrive at the pseudo-steady state approximation of the maximal soluble drug concentration in the tissue [33] (Eq. 2T) as,

$$C_{max} \approx k_c^T (L/D)C_s. \quad [2T]$$

The superscript T denotes the tissue value of the mass transfer coefficient. Numerical simulations that also account for cell uptake and drug binding to extracellular proteins and intracellular receptors confirmed the high accuracy of Eqs. 1T and 2T in all the scenarios we considered.

2.3 Apparent coating clearance kinetics

Denoting the mass of the tissue embedded coating as *its* dissolution area as A^T we obtain,

$$\frac{dM^T}{dt} = A^T \cdot (\text{tissue dissolution flux}). \quad [3T]$$

In contrast, the lumenal adherent coating dissolves both at its blood-contacting surface (A^L) and its tissue-contacting surface (A^T) so that

$$\frac{dM^L}{dt} = A^L \cdot (\text{lumenal dissolution flux}) - A^T \cdot (\text{tissue dissolution flux}) \approx \quad A^L \quad [3L]$$

$\cdot (\text{lumenal dissolution flux}),$

The last approximation builds on the fact that while the surface areas A^L and A^T of the lumenal adherent coating will be approximately equivalent the lumenal dissolution flux is expected to be much higher than the tissue dissolution flux emanating from this coating.

To facilitate the interpretation of *in vivo* experiments we introduce the weight based concentrations of lumenal (S^L) and tissue (S^T) coating, obtained by dividing the weight of the solid drug by the weight of the tissue ($\rho\, V_{tiss}$), where ρ is the density of the tissue (0.98 µg/mL [37]) and V_{tiss} is its volume. Building on the rate equations for the coating masses (Eqs. 3L and 3T) and substituting the approximations of lumenal and tissue fluxes (Eqs. 1L and 1T) we obtain the following rate equations for the weight based coating concentrations

$$dS^L/dt \approx A^L \cdot (\text{lumenal dissolution flux}) \approx -k^L(C_s/\rho), \quad [4L]$$

$$\frac{dS^T}{dt} = -A^T \cdot (\text{tissue dissolution flux}) \approx -k^T(C_s/\rho). \quad [4T]$$

Her $k^L = (A^L/V_{tiss}) \cdot k_c^L$ and $K^T = (A^T/V_{tiss}) \cdot k_c^T$ are the respective apparent dissolution rate constants in the lumen and tissue. Hence, the concentrations of lumenal and tissue embedded coating are both predicted to decrease linearly over time, with the former depleting at time T_L as

$$S^L \approx S_0^L\left(1 - \frac{t}{T_L}\right), T_L = \frac{S_0^L}{k^L(C_s/\rho)} \quad [5L]$$

and the latter depleting at time $T_T > T_L$ as

$$S^T \approx S_0^T\left(1 - \frac{t}{T_T}\right), T_T = \frac{S_0^T}{k^T(C_s/\rho)}. \quad [5T]$$

3. Results

3.1 Paclitaxel coating retention and tissue dosing

Taken together, Eqs. 5L and 5T imply that apparent coating concentration will decline with piecewise time-linear kinetics reflecting perhaps the differential mass transfer rate constants of the drug at the lumenal surface and deep in the tissue

$$S_{tissue} \approx \begin{cases} S_0^L + S_0^T - (k^L + k^T)(C_s/\rho) \cdot t, & 0 < t < T_L \\ S_0^T - k^T(C_s/\rho) \cdot (t - T_L), & T_L < t < T_T \end{cases}. \quad [6]$$

Segmental linear regression of *in vivo* bulk tissue content data confirms that Eq. 6 holds remarkably well (Table 1) for PCB primarily coated with a single paclitaxel polymorph (first three formulations) and those with unknown or mixed composition (Ranger™ and Lutonix®). The estimated lifetimes of the lumenal coating (T^L) ranged from 1–4.5d, with the lowest solubility polymorph (dihydrate) producing longest lifetimes. However, no clear trend on polymorph solubility was observed, perhaps implying that the regression significantly over-estimates the lifetime (T^L) of the lumenal amorphous coating owing to insufficient data granularity. The estimated lifetimes of the tissue embedded coating ranged from 41 to 221 days, with no clear dependence on solubility or the magnitude of the tissue embedded pool (S_0^T). Surprisingly a small fraction of the amorphous coating was estimated to reside up to 43.7d in the tissue, similar to the lifetimes of the dihydrate coated PCB, IN.PACT and Ranger. Paclitaxel retention for the Lutonix PCB is qualitatively similar to that of the Amorphous coated PCB, in that the majority of the coating delivered by both is fast

clearing, but a small fraction is predicted to be very stable and long residing (44d for Amorphous, 221d for Lutonix). Of all the analyzed cases, IN.PACT™ and Ranger exhibited the most similar delivery profile, with both delivering the majority of the coating to the lumen with a lifetime of 1.4 days and sizable minority of the coating to the tissue with a lifetime of, respectively, 46.7 and 41.7 days.

The full power of Eq. 6 becomes evident when it is used to predict the maximal sustained concentration of soluble drug in the tissue, $C_{max,}$ (Table 1). This is achieved by rewriting C_{max} as defined in Eq. 2T, in terms of the apparent dissolution rate-constant k^T

$$C_{max} = \frac{k_c^T}{(D/L)}C_s = \frac{k^T}{(D/L^2)}C_s \quad [7]$$

and inserting this into the approximate kinetic equation describing coating dissolution,

$$S^T = S_0^T - k^T(C_s/\rho) \cdot (t - T_L) = S^T = S_0^T - (D/L^2)(C_{max}/\rho) \cdot (t - T_L). \quad [8]$$

This allows for the inference of C_{max} directly from estimated pre-factor of the shifted time term $(t-T_L)$ in Eq. 6. These estimates are reported in Table 1 as $Cmax,sus$ to highlight the fact that they are valid up to depletion of the tissue embedded coating at time T^T. The dihydrate and anhydrous coated PCB are both predicted to sustain nanomolar concentrations in the tissue, with Ranger predicted to sustain a very similar concentration to IN.PACT. The amorphous paclitaxel coating and the Lutonix coating are both predicted to sustain a sub nanomolar concentration.

3.2   Receptor-binding dictates distribution and retention dynamics

The predicted maximal soluble drug concentrations are low compared to the affinity of extracellular binding site for paclitaxel (3–136 μM[34, 35]) suggesting that low affinity binding sites are far from saturation and play a minor role in retaining paclitaxel. If confirmed, this provides an opportunity to estimate the concentration of paclitaxel receptors from retention dynamics post coating depletion. This is illustrated in the analysis of IN.PACT data below.

3.2.1   Anhydrous paclitaxel coating—The IN.PACT PCB is coated primarily with anhydrous paclitaxel and *in vitro* dissolution kinetics are consistent with a single polymorph[21]. *In vivo* tissue retention of the IN.PACT coating follows piecewise linear kinetics (Eq. 6) up to 45d post inflation in porcine iliofemoral arteries, allowing the estimation of the dissolution rate constants of lumenal and tissue embedded anhydrous paclitaxel coatings (Table 2).

However, whereas the piecewise linear fit predicts complete coating dissolution by ~45d, paclitaxel levels in the tissue remain measurable up to 60d (Figure 4A). In principle this discrepancy may reflect that the coating morphology is not pure as assumed and includes a

small slow dissolving fraction, However, this seems unlikely given the qualitative change in kinetics beyond 45d (namely an additional slow component would simply shift the blue curve in Figure 4A to the right). Alternatively, the slow decline after 45d might be due to the slower clearance of drug bound to high affinity receptors, similar to drug-eluting stents[30, 39]). Indeed, as the piecewise linear fit is insensitive to constant shifts, it seems likely that tissue levels at 45d (0.4 ng/mg) are associated with dissolved drug (Figure 4A), which would imply that coating is already fully dissolved by this time. To examine this interpretation we numerically simulated transmural drug distribution subject to dissolution boundary conditions (Eq. 1) with the anhydrous paclitaxel dissolution rate constants (Table 2) and experimentally estimated tissue diffusion and non-specific binding constants in porcine iliofemoral arteries[35].

Simulated soluble drug concentrations at the coating-tissue interface reached 89% maximal concentration ($0.89 \cdot C_{max}$) within the first hour, and thereafter only slowly approached the maximal equilibrium level (C_{max} = 1.3 nM) (Figure 4B), as cells slowly siphoned extracellular drug. Simulated bulk tissue concentrations of dissolved paclitaxel mirrored this trend and closely tracked the bulk tissue concentration of receptor-bound drug (Figure 4C) as only a miniscule fraction of low affinity binding sites were drug-bound. Receptor-bound drug dominated tissue retention of soluble drug even more once the coating had fully dissolved with sustained drug in the tissue beyond 60d (Figure 4C). This was true as the concentration of receptors was progressively ramped up to $B_{rec,max}$=4.2 μM so as to match *in vivo* paclitaxel concentrations at 45 and 60d. Tissue content levels are predicted to reach a 0.01 ng/mg lower limit of detection at 94.5d. While high affinity binding of paclitaxel to microtubules is predicted to mediate sustained drug retention after coating dissolution, it is important to note that in cell-culture studies with human endothelial and smooth muscle cells, ultralow paclitaxel concentrations that did not affect microtubule assembly inhibited proliferation with IC_{50} = 0.1 pM[18] (8.7×10^{-8} ng/mg drug/tissue) and migration with IC_{50} = 1 pM[19] (8.7×10^{-7} ng/mg drug/tissue). As such, the concentration of extracellular drug provides an independent computational predictor of biological effects in the tissue, particularly when $> 1 \times 10^{-6}$ ng/mg. For anhydrous paclitaxel coating in healthy porcine iliofemoral arteries this is predicted to occur at 102d.

3.2.2 Dihydrate paclitaxel coating—Data on the *in vivo* retention of paclitaxel in dihydrate coated PCB treated rabbit aorta[38] are notable for the slow dissolution of the lumenal coating which persists for 4.5d and a sustained plateau between 7 and 28d owing to the slow dissolution of the tissue embedded coating (Figure 5A). Simulations using the dihydrate paclitaxel dissolution parameters (Table 2) and the same diffusion coefficient and receptor binding parameters as for porcine iliofemoral arteries predicted the contribution of dissolved drug to tissue retention. The concentration of non-specific binding sites was adjusted to the measured partition coefficient of paclitaxel in rabbit aorta, which is 1.9-fold higher than in porcine iliofemoral arteries[36]. Despite some differences in parameter values, the predicted trends were similar to those in porcine arteries. Simulated soluble drug concentrations at the coating-tissue interface reached 89% maximal concentration ($0.89 \cdot C_{max}$) within the first hour, and thereafter only slowly approached the maximal equilibrium level (C_{max} = 4.3 nM) (Figure 5B), as cells slowly siphoned extracellular drug.

Simulated bulk tissue concentrations of dissolved paclitaxel mirrored this trend and closely tracked the bulk tissue concentration of receptor-bound drug (Figure 5C) as only a miniscule fraction of low affinity binding sites were drug-bound. Receptor-bound drug dominated tissue retention of soluble paclitaxel even more once the coating was predicted to have fully dissolved by ~ 60d and sustained drug in the tissue through 90d (Figure 5C). Notably, concentrations of receptors inferred from IN.PACT treated porcine iliofemoral arteries ($B_{rec,max}$=4.2 μM) adequately predicted paclitaxel retention in rabbit aorta. Tissue content levels are predicted to reach a 0.01 ng/mg lower limit of detection at ~120d and average soluble extracellular concentrations to remain $> 1 \times 10^{-6}$ ng/mg for ~130d.

3.3 Hindered diffusivity elevates the dosing concentration and prolongs retention

Paclitaxel diffusion in dense and calcified plaque is significantly hindered relative to diffusion in healthy animal arteries, potentially up to 300-fold[42]. Hence, for clinical relevance it is informative to evaluate the influence of reducing the diffusion coefficient 10- and 100-fold compared to the healthy animal baseline. Based on the estimated dissolution rate constant of anhydrous paclitaxel (Table 2) the IN.PACT coating, 10- and 100-fold reductions in diffusivity extend coating dissolution time (T^T, Eq. 5T) by only 0.2 and 1.7d, respectively, while increasing the maximal dosing concentration 10- and 96-fold and the fraction of bound receptors 4.5- and 7.6-fold, respectively. Consequently, receptor-mediated retention of dissolved drug is substantially prolonged, with predicted detectable tissue levels (>0.01 ng/mg) up to 210d for a 10-fold diffusive hindrance (Figure 6A) and up to 3 years for a 100fold diffusive hindrance (Figure 6B). Notably, free extracellular paclitaxel concentration is predicted to exceed 1×10^{-6} ng/mg even as the average tissue concentration declines below 0.01 ng/mg (Figure 6A,B).

DISCUSSION

Much that we know about arterial drug distribution and biological effects has been gained through experience with drug release from durable polymer coated stents wherein device explant allows for measurement of residual drug in the coating and in the subjacent tissue. Such neat separation is no longer possible for absorbable coatings that deploy into the tissue and created the need for the development of new techniques for interpreting the local pharmacokinetics of coating delivery devices. This class of endovascular drug delivery devices has been gaining popularity in clinical practice and includes drug-coated balloons, a sub-class of polymer free drug-coated stents such as the Zilver PTX, nano-particulate coated balloons and stents and the MiStent with its absorbable polymer coating and embedded crystalline drug load. For each of these devices, drug release is no longer synonymous with elution of soluble drug, making it hard to infer the amount of pharmacologically active drug in the tissue based on measured bulk *in vivo* tissue content. Moreover, in contrast to stents where the entire drug load abuts the tissue and locally releases drug, PCB only deliver a small fraction (~10–15%) of their drug load locally to the subjacent artery, with some adhering to the lumenal aspect and the rest distributing into the wall. Given this relative lack of control over dosing it has been difficult to unravel the contributions of coating design, procedural parameters and lesion complexity to tissue dosing levels and kinetics. This has been further complicated by the fact that while solid coating dominates experimental tissue

retention data, it is the solubilized drug that exerts biological effects in the tissue. To address these challenges, we rely on mechanistic computational modeling.

Determinants of local dosing and retention of soluble drug

The current computational analysis reiterates and quantifies the importance of coating parameters determining the rate of its dissolution, while providing new insights into the importance of tissue diffusivity in determining dosing levels and persistence via the inverse dependence of the maximal concentration of soluble drug in the tissue on the transmural diffusion rate. As a result of diffusion, model predicted concentrations of soluble extracellular paclitaxel in healthy animal arteries are in the nanomolar range, 3-orders of magnitude lower than would be implied by the solubility of paclitaxel. Nevertheless, owing to the nanomolar affinities of paclitaxel to its intracellular receptors (microtubules), such levels of solubilized drug are sufficient to saturate a sizable fraction of receptors in the tissue during coating dissolution, providing receptor mediated effects and sustained retention after depletion of solid drug depots in the tissue.

Indeed, it is this dependence of late retention on receptor binding that has allowed us to estimate the concentration of paclitaxel receptors in healthy porcine iliofemoral arteries (3.7 ng receptors/g tissue) as well as the persistence of solid drug in these arteries (45 d). The former is only 20% higher than the estimated concentration of sirolimus receptors in coronary arteries (3.0 ng receptors/g tissue [30]), whereas the latter is 4-fold longer than *in vitro* dissolution of the same coating in pig plasma[21]. Slower *in vivo* coating dissolution is consistent with the exposure of tissue embedded coating to slower convection relative to *in vitro* dissolution experiments. Indeed, one would expect the disparity between *in vitro* and *in vivo* dissolution rates of the same coating to be even larger, suggesting that *in vitro* dissolution experiments assessed the dissolution of IN.PACT coating that embolizes rather than that which is transferred into the tissue. This could potentially explain histological observations of this coating in downstream skeletal muscle up to 90d, long after crystals were no longer observed at the treatment site[43]. Thus, concerns for potential late toxicity owing to slow release of paclitaxel from coating emboli are reflective of possible local toxicities for a particular subset of coating formulations and morphologies, not a class effect of crystalline coated PCB.

Clinical implications for paclitaxel coated balloons

The presented analysis provides a theoretical underpinning for the ability of paclitaxel coating to sustain delivery of therapeutic drug doses to arteries over long times. Importantly, the degree of dosing depends not only on the amount of delivered coating and its solubility, but also on the distance of the coating particles from the lumen and on the permeability of the tissue. Particles closer to the lumen will be exposed to greater washout and therefore dissolve more quickly. By contrast, slower diffusion in diseased arteries may lead to slower particle dissolution and higher soluble drug concentrations in the tissue. Thus, diseased arteries may hinder coating from penetrating beyond the mineralized intima, thereby limiting drug exposure to the underlying tissue, while allowing coating to lodge deeper into non-mineralized but lower permeability areas that promote sustained local tissue exposure at near solubility levels. Given the spatial variability in the composition, mechanical properties

and permeability of diseased tissue, tissue regions of late drug retention might be small and not even be apparent in macroscopic measurements of drug content. Yet even focal regions of late retention are biologically significant, illustrating the power of quantitative reasoning to highlight concern that may elude conventional experimental techniques. This dependence of tissue dosing kinetics on tissue compliance and permeability implies a dependence on coating morphology (e.g. particle size and shape) and therefore speaks to a lack of a class effect. By the same token, it highlights the importance of procedural parameters that modulate local tissue compliance and permeability to drug, e.g. balloon inflation time, pressure and balloon to artery ratio, and other more sophisticated adjunctive vessel preparation technologies.

Taken together, the current analysis provides a potential theoretical explanation for the persistent anti-restenotic effects of PCB for up to several years post treatment owing to slow dissociation of paclitaxel from its pharmacological receptor, and concomitantly low soluble drug concentrations that are unlikely to be toxic locally. At the same time, drug bound for months to years possibly exerting a durable local effect could have off-target effects over time. However, this would require that drug solubilized into the flowing blood stream in peripheral arteries would then make its way through the entire circulation including the lungs to lodge in other tissues, penetrate, bind and be retained in biologically active form – an unlikely combination of occurrences.

Relevance to sirolimus coated balloons and stents

Similar to paclitaxel, sirolimus is a highly lipophilic small molecule that inhibits cell proliferation and migration through high affinity binding to intracellular receptors. These attributes and its wider therapeutic window compared to paclitaxel have allowed sirolimus analogs to supersede paclitaxel as the drugs of choice for elution from coronary stents. In contrast, the formulation chemistry of PCB with its reliance on excipients to optimize drug transfer and retention does not seem to be applicable to sirolimus. However, alternative strategies for crystalline sirolimus delivery have been developed that show promise in sustaining tissue dosing in arterial tissue. In lieu of chemistry based formulation strategies for reducing the dissolution rate of sirolimus crystals, encapsulation within polymer coatings on stents or balloons has emerged as a promising alternative for achieving this goal. This is because loading of crystalline drug into a polymer isolates the drug particles from direct contact with blood or tissue, thereby ensuring that the thickness of the stagnant boundary layer abutting solid drug particles is insensitive to the differences in ambient convective forces and that lumenal dissolution is tempered. This explains our earlier findings on the MiStent, where we showed that the sirolimus microcrystals remaining on the stent and embedded into the tissue owing to coating deployment all dissolved at the same constant rate over the course of 90d [17, 44].

Limitations and future directions

Several geometric and kinetic assumptions underlying the current analysis should be revisited and informed by additional experimental data when considering a more complete description of dissolution controlled endovascular drug delivery stents. First, for simplicity, the model focused on the case of homogeneous crystalline coatings comprised of a dominant

solid form. This assumption is easily relaxed, but requires specific and detailed information on coating formulation that is currently unreported in the literature. Our hope is that this work will encourage the reporting of coating composition in terms of the percentages of paclitaxel polymorphs rather than drug and excipient loads. In addition, the assumption that lumen-adherent coating does not contribute to dosing is based on a time scale argument that is invalid for amorphous coatings and coatings that, include a fast dissolving component, like the Lutonix PCB or the Zilver PTX (or the recently approved Eluvia stent owing to the incorporation of paclitaxel into a durable polymer coating). Such coating components that dissolve within minutes in plasma[21, 35] likely also quickly dissolve on their tissue contacting side and diffuse into the tissue concomitant with blood clearance on their lumenal aspect and can be modeled using the same tissue transport equations but with different boundary conditions[35]. This was not pursued in the current study owing to the lack of early data on dissolution and or compositional information. Moreover, the assumption of mass transfer limited dissolution can break down for such amorphous drug components, leading to the possibility of solvent mediated conversion to the most stable drug polymorph[45, 46]. Indeed, this theoretical possibility is supported by preclinical evidence that amorphous coated PCB and the Lutonix PCB both give rise to a very small fraction of sustainably retained tissue delivered coating. By contrast, our analysis indicates that phase mediated interconversion of anhydrous paclitaxel into the more stable dihydrate form is extremely unlikely owing to the fast diffusive clearance of paclitaxel at the coating-tissue interface, as this does not allow time for crystallization[45]. Geometric simplifications were related to the assumed distribution of lumenal and tissue embedded coating. For the purposes of a general systems understanding, simulations considered an ideal situation wherein lumenal coating is spread across the entire treated lumenal interface. Yet published images of fluorescent drug distribution on the mural interface show inhomogeneities[24] as does our own unpublished work. Similarly, the assumption that tissue embedded coating remains close to the lumen is also an over-simplification, especially at later times. Consequently, the approximation of the diffusion rate as D/L^2 is a lower bound estimate. Future preclinical evaluations of novel devices of this class would therefore benefit from the use of imaging techniques to better characterize coating distribution at the lumen and within the tissue. Incorporation of such patterns into computational models[17] would then allow for more quantitatively and spatially accurate predictions of tissue dosing.

Conclusions

The notable clinical efficacy of paclitaxel coated balloons and stents in the treatment of femoropopliteal arterial disease was achieved on the basis of an empiric appreciation that sustained drug retention is requisite for ensuring persistent inhibition of intimal hyperplasia. Remarkably, clinical efficacy was achieved on the basis of only scant appreciation of the determinants of local distribution and retention of drug and its partitioning between solid coating, solubilized free and bound extracellular and intracellular drug. This state of affairs has hampered the adoption of these devices to other vascular beds and is no longer acceptable now that the question of their safety has come under renewed scrutiny despite the absence of a putative mechanism for elevated mortality. Faced with this crisis we must seek new methods and tools for understanding and controlling local drug delivery from these and related devices. As we have illustrated herein, computational modeling provides a flexible

quantitative framework for explaining data obtained in healthy animals, while offering unique insights into the influence of, not only coating design parameters, but also of tissue morphologies typical of the very disease states which these devices seek to treat. In a fascinating way, mineralization which was long held to only limit the efficacy of these devices via hindrance of drug distribution into artery wall, is now shown to also provide a mechanism for sustained local retention owing to hindered diffusive clearance of drug.

Supplementary Material

Refer to Web version on PubMed Central for supplementary material.

Acknowledgements

References

[1]. Li J, Parikh SA, Drug-coated balloons for long lesions in peripheral arterial disease, The Journal of cardiovascular surgery, 58 (2017) 698–714. [PubMed: 28530090]

[2]. Axel DI, Kunert W, Goggelmann C, Oberhoff M, Herdeg C, Kuttner A, Wild DH, Brehm BR, Riessen R, Koveker G, Karsch KR, Paclitaxel inhibits arterial smooth muscle cell proliferation and migration in vitro and in vivo using local drug delivery, Circulation, 96 (1997) 636–645. [PubMed: 9244237]

[3]. Levin AD, Vukmirovic N, Hwang CW, Edelman ER, Specific binding to intracellular proteins determines arterial transport properties for rapamycin and paclitaxel, Proceedings of the National Academy of Sciences of the United States of America, 101 (2004) 9463–9467. [PubMed: 15197278]

[4]. Speck U, Stolzenburg N, Peters D, Scheller B, How does a drug-coated balloon work? Overview about coating technologies and their impact, The Journal of cardiovascular surgery, (2015).

[5]. Chao Y, Chan WK, Birkhofer MJ, Hu OY, Wang SS, Huang YS, Liu M, Whang-Peng J, Chi KH, Lui WY, Lee SD, Phase II and pharmacokinetic study of paclitaxel therapy for unresectable hepatocellular carcinoma patients, British journal of cancer, 78 (1998) 34–39. [PubMed: 9662247]

[6]. Liggins RT, Hunter WL, Burt HM, Solid-state characterization of paclitaxel, Journal of pharmaceutical sciences, 86 (1997) 1458–1463. [PubMed: 9423162]

[7]. Que C, Gao Y, Raina SA, Zhang GGZ, Taylor LS, Paclitaxel Crystal Seeds with Different Intrinsic Properties and Their Impact on Dissolution of Paclitaxel-HPMCAS Amorphous Solid Dispersions, Crystal Growth & Design, 18 (2018) 1548–1559.

[8]. Granada JF, Stenoien M, Buszman PP, Tellez A, Langanki D, Kaluza GL, Leon MB, Gray W, Jaff MR, Schwartz RS, Mechanisms of tissue uptake and retention of paclitaxel-coated balloons: impact on neointimal proliferation and healing, Open heart, 1 (2014) e000117. [PubMed: 25332821]

[9]. Reyes P, Moore WF, NMyers RJ, Ruane PH, Morrell MS, Methods of manufacturing and modifying taxane coatings for implantable medical devices, in, MED Institute Inc Cook Medical Technologies LLC USA, 2011.

[10]. Kangas S, Chen Y-L, Use of Drug Polymorphs to Achieve Controlled Drug Delivery From a Coated Medical Device, in, Boston Scientific Scimed Inc USA, 2010.

[11]. Speck U, Drug-Eluting Medical Device, in, INVATEC TECHNOLOGY CENTER GMBH, Frauenfeld (CE), 2010.

[12]. Speck U, Schaffner S, Renke-Gluszko M, DRUG - ELUTING MEDICAL DEVICE in: USAPT (Ed.), Invatec Technology Center GMBH, Frauenfeld (CH), USA, 2018.

[13]. Katsanos K, Spiliopoulos S, Kitrou P, Krokidis M, Karnabatidis D, Risk of Death Following Application of Paclitaxel-Coated Balloons and Stents in the Femoropopliteal Artery of the Leg: A Systematic Review and Meta-Analysis of Randomized Controlled Trials, Journal of the American Heart Association, 7 (2018) e011245. [PubMed: 30561254]

[14]. Secemsky EA, Kundi H, Weinberg I, Jaff MR, Krawisz A, Parikh SA, Beckman JA, Mustapha J, Rosenfield K, Yeh RW, Association of Survival With Femoropopliteal Artery Revascularization With Drug-Coated Devices, JAMA cardiology, (2019).

[15]. Schneider PA, Laird JR, Doros G, Gao Q, Ansel G, Brodmann M, Micari A, Shishehbor MH, Tepe G, Zeller T, Mortality Not Correlated with Paclitaxel Exposure: An Independent Patient-level Meta-Analysis, Journal of the American College of Cardiology, (2019).

[16]. Gongora CA, Shibuya M, Wessler JD, McGregor J, Tellez A, Cheng Y, Conditt GB, Kaluza GL, Granada JF, Impact of Paclitaxel Dose on Tissue Pharmacokinetics and Vascular Healing: A Comparative Drug-Coated Balloon Study in the Familial Hypercholesterolemic Swine Model of Superficial Femoral In-Stent Restenosis, JACC. Cardiovascular interventions, 8 (2015) 1115–1123. [PubMed: 26117470]

[17]. Tzafriri AR, Garcia-Polite F, Li X, Keating J, Balaguer JM, Zani B, Bailey L, Markham P, Kiorpes TC, Carlyle W, Edelman ER, Defining drug and target protein distributions after stent-based drug release: Durable versus deployable coatings, Journal of controlled release : official journal of the Controlled Release Society, 274 (2018) 102–108. [PubMed: 29421608]

[18]. Wang J, Lou P, Lesniewski R, Henkin J, Paclitaxel at ultra low concentrations inhibits angiogenesis without affecting cellular microtubule assembly, Anti-cancer drugs, 14 (2003) 13–19. [PubMed: 12544254]

[19]. Hou D, Huibregtse BA, Eppihimer M, Stoffregen W, Kocur G, Hitzman C, Stejskal E, Heil J, Dawkins KD, Fluorocopolymer-coated nitinol self-expanding paclitaxel-eluting stent: pharmacokinetics and vascular biology responses in a porcine iliofemoral model, EuroIntervention : journal of EuroPCR in collaboration with the Working Group on Interventional Cardiology of the European Society of Cardiology, 12 (2016) 790–797.

[20]. Dake MD, Van Alstine WG, Zhou Q, Ragheb AO, Polymer-free paclitaxel-coated Zilver PTX Stents--evaluation of pharmacokinetics and comparative safety in porcine arteries, Journal of vascular and interventional radiology : JVIR, 22 (2011) 603–610. [PubMed: 21419649]

[21]. Granada JF, Virmani R, Schulz-Jander D, Tunev S, Melder RJ, Rate of Drug Coating Dissolution Determines In-Tissue Drug Retention and Durability of Biological Efficacy, Journal of Drug Delivery, 2019 (2019) 7.

[22]. Yazdani SK, Pacheco E, Nakano M, Otsuka F, Naisbitt S, Kolodgie FD, Ladich E, Rousselle S, Virmani R, Vascular, downstream, and pharmacokinetic responses to treatment with a low dose drug-coated balloon in a swine femoral artery model, Catheterization and cardiovascular interventions : official journal of the Society for Cardiac Angiography & Interventions, 83 (2014) 132–140. [PubMed: 23703778]

[23]. Schorn I, Malinoff H, Anderson S, Lecy C, Wang J, Giorgianni J, Papandreou G, The Lutonix(R) drug-coated balloon: A novel drug delivery technology for the treatment of vascular disease, Advanced drug delivery reviews, 112 (2017) 78–87. [PubMed: 28559093]

[24]. Cheng Y, Leon MB, Granada JF, An update on the clinical use of drug-coated balloons in percutaneous coronary interventions, Expert opinion on drug delivery, 13 (2016) 859–872. [PubMed: 26924794]

[25]. Levich VG, Physiochemical Hydrodynamics, Prentice-Hall, Englewood Cliffs, N. J., 1962.

[26]. Melder RJ, IN.PACT DEB technology and Pre-clinical Science, in: LINC, 2012.

[27]. Krishnan P, Faries P, Niazi K, Jain A, Sachar R, Bachinsky WB, Cardenas J, Werner M, Brodmann M, Mustapha JA, Mena-Hurtado C, Jaff MR, Holden AH, Lyden SP, Stellarex Drug-Coated Balloon for Treatment of Femoropopliteal Disease: Twelve-Month Outcomes From the

Randomized ILLUMENATE Pivotal and Pharmacokinetic Studies, Circulation, 136 (2017) 1102–1113. [PubMed: 28729250]

[28]. Kumar GN, Walle UK, Bhalla KN, Walle T, Binding of taxol to human plasma, albumin and alpha 1-acid glycoprotein, Research communications in chemical pathology and pharmacology, 80 (1993) 337–344. [PubMed: 8102493]

[29]. Lovich MA, Creel C, Hong K, Hwang CW, Edelman ER, Carrier proteins determine local pharmacokinetics and arterial distribution of paclitaxel, Journal of pharmaceutical sciences, 90 (2001) 1324–1335. [PubMed: 11745785]

[30]. Tzafriri AR, Groothuis A, Price GS, Edelman ER, Stent elution rate determines drug deposition and receptor-mediated effects, Journal of controlled release : official journal of the Controlled Release Society, 161 (2012) 918–926. [PubMed: 22642931]

[31]. Tzafriri AR, Lerner EI, Flashner-Barak M, Hinchcliffe M, Ratner E, Parnas H, Mathematical modeling and optimization of drug delivery from intratumorally injected microspheres, Clinical cancer research : an official journal of the American Association for Cancer Research, 11 (2005) 826–834. [PubMed: 15701873]

[32]. Indolfi L, Ligorio M, Ting DT, Xega K, Tzafriri AR, Bersani F, Aceto N, Thapar V, Fuchs BC, Deshpande V, Baker AB, Ferrone CR, Haber DA, Langer R, Clark JW, Edelman ER, A tunable delivery platform to provide local chemotherapy for pancreatic ductal adenocarcinoma, Biomaterials, 93 (2016) 71–82. [PubMed: 27082874]

[33]. Crank J, Diffusion in a plane sheet, in: The Mathematics of Diffusion, Clarendon Press, Oxford, 1975, pp. 44–45.

[34]. Tzafriri AR, Levin AD, Edelman ER, Diffusion-limited binding explains binary dose response for local arterial and tumour drug delivery, Cell proliferation, 42 (2009) 348–363. [PubMed: 19438899]

[35]. Kolachalama VB, Pacetti SD, Franses JW, Stankus JJ, Zhao HQ, Shazly T, Nikanorov A, Schwartz LB, Tzafriri AR, Edelman ER, Mechanisms of tissue uptake and retention in zotarolimus-coated balloon therapy, Circulation, 127 (2013) 2047–2055. [PubMed: 23584359]

[36]. Tzafriri AR, Vukmirovic N, Kolachalama VB, Astafieva I, Edelman ER, Lesion complexity determines arterial drug distribution after local drug delivery, Journal of controlled release : official journal of the Controlled Release Society, 142 (2010) 332–338. [PubMed: 19925836]

[37]. Lovich MA, Edelman ER, Tissue average binding and equilibrium distribution: an example with heparin in arterial tissues, Biophysical journal, 70 (1996) 1553–1559. [PubMed: 8785313]

[38]. Granada JF, The Next Generation of Drug-Coated Balloons: The Ranger Paclitaxel-Coated PTA Balloon Catheter, INSERT TO ENDOVASCULAR TODAY EUROPE, 2 (2014) 2–5.

[39]. Artzi N, Tzafriri AR, Faucher KM, Moodie G, Albergo T, Conroy S, Corbeil S, Martakos P, Virmani R, Edelman ER, Sustained Efficacy and Arterial Drug Retention by a Fast Drug Eluting Cross-Linked Fatty Acid Coronary Stent Coating, Annals of biomedical engineering, 44 (2016) 276–286. [PubMed: 26314990]

[40]. Tarr BD, Yalkowsky SH, A new parenteral vehicle for the administration of some poorly water soluble anti-cancer drugs, Journal of parenteral science and technology : a publication of the Parenteral Drug Association, 41 (1987) 31–33. [PubMed: 3559832]

[41]. Swindell CS, Krauss NE, Horwitz SB, Ringel I, Biologically active taxol analogues with deleted A-ring side chain substituents and variable C-2' configurations, Journal of medicinal chemistry, 34 (1991) 1176–1184. [PubMed: 1672157]

[42]. Tzafriri AR, Garcia-Polite F, Zani B, Stanley J, Muraj B, Knutson J, Kohler R, Markham P, Nikanorov A, Edelman ER, Calcified plaque modification alters local drug delivery in the treatment of peripheral atherosclerosis, Journal of controlled release : official journal of the Controlled Release Society, 264 (2017) 203–210. [PubMed: 28867375]

[43]. Kolodgie FD, Pacheco E, Yahagi K, Mori H, Ladich E, Virmani R, Comparison of Particulate Embolization after Femoral Artery Treatment with IN.PACT Admiral versus Lutonix 035 Paclitaxel-Coated Balloons in Healthy Swine, Journal of vascular and interventional radiology : JVIR, 27 (2016) 1676–1685 e1672. [PubMed: 27641674]

[44]. Carlyle WC, McClain JB, Tzafriri AR, Bailey L, Zani BG, Markham PM, Stanley JR, Edelman ER, Enhanced drug delivery capabilities from stents coated with absorbable polymer and

crystalline drug, Journal of controlled release : official journal of the Controlled Release Society, 162 (2012) 561–567. [PubMed: 22800575]

[45]. Nogami H, Nagai T, Yotsuyanagi T, Dissolution Phenomena of Organic Medicinals involving Simulatneaous Phase Changes, Chemical & pharmaceutical bulletin, 17 (1969) 499–508.

[46]. Cardew PT, Davey RJ, The kinetics of solvent-mediated phase transformations, Proc. R. Soc. Lond. A, 398 (1985) 415–428.
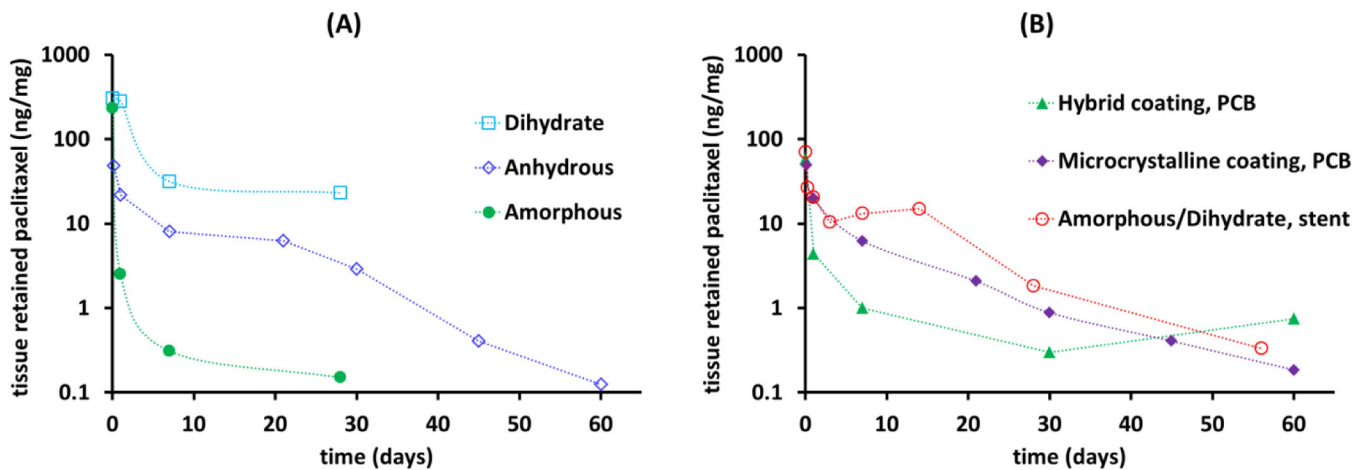
Figure 1.
Local arterial retention of paclitaxel in healthy animal arteries after inflation of devices coated with pure forms of amorphous or crystalline paclitaxel (A) or mixed forms (B). Data compiled from peer reviewed publications [8, 20–23].
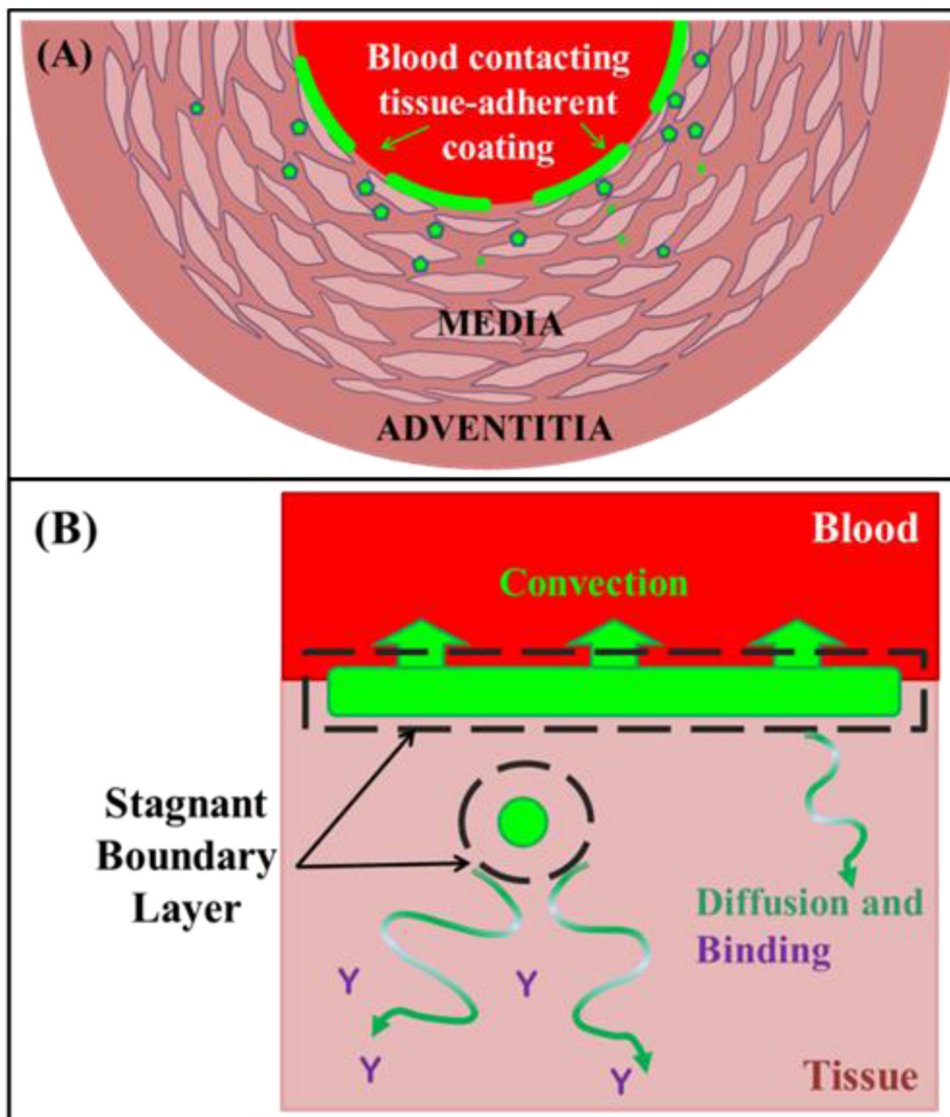
Figure 2.
Schematic geometry. (A) Balloon delivered coating either adheres as patches to the lumenal surface (dashes) or as particulates that embed into the tissue (symbols). Surface adherent coating is bounded by blood on one side and by tissue on the other, with each surface dissolving at a rate dictated by ambient transport forces. (B) Coating dissolution occurs via solubilization into a thin stagnant layer at the boundary (dashes) of which soluble drug is removed via local transport forces: convection at the lumenal aspect and diffusion within the tissue.
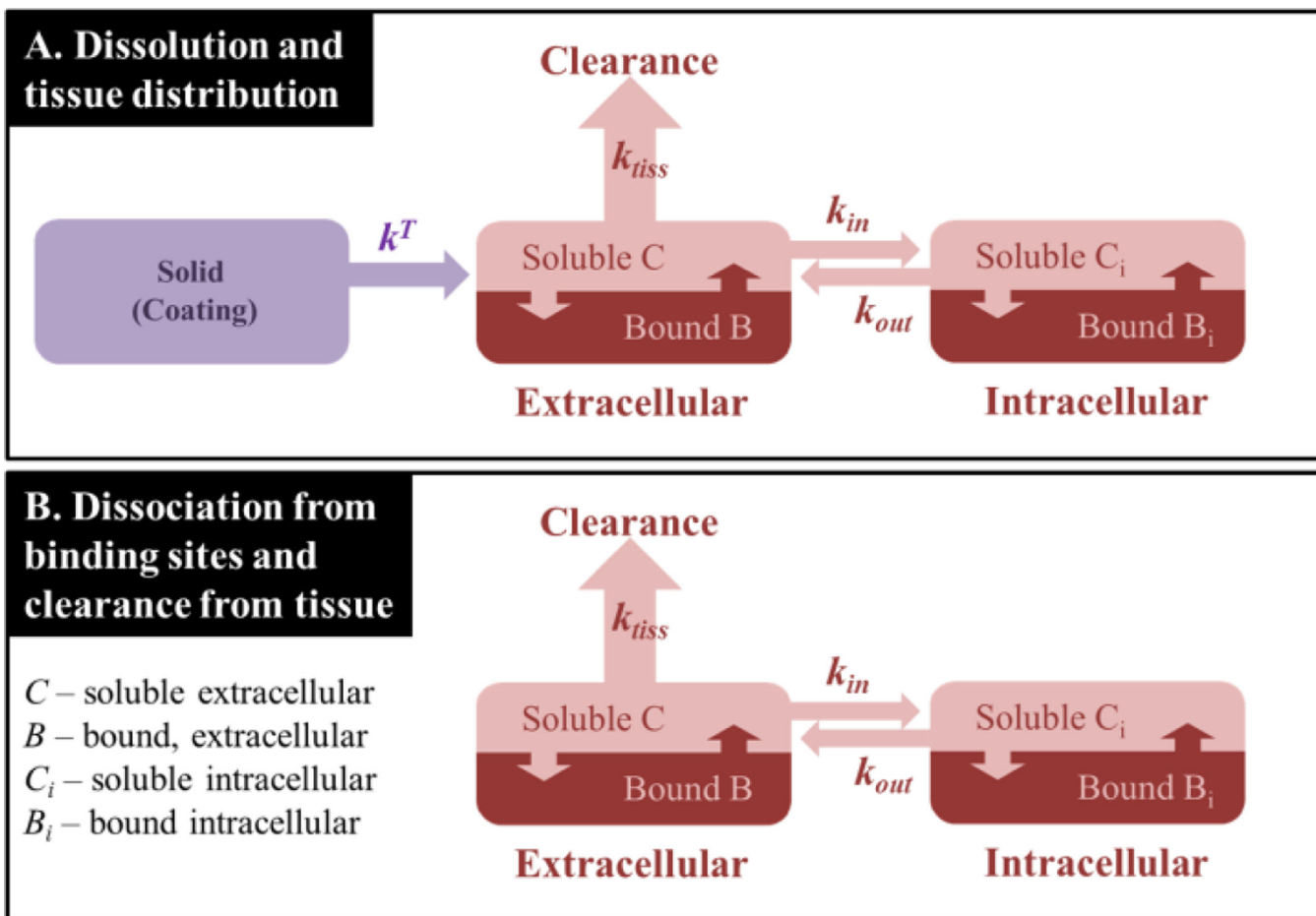
A. Dissolution and tissue distribution

Clearance

k_{tiss}

Solid (Coating) $\xrightarrow{k^T}$ Soluble C / Bound B — k_{in} / k_{out} — Soluble C_i / Bound B_i

Extracellular   Intracellular

B. Dissociation from binding sites and clearance from tissue

C – soluble extracellular
B – bound, extracellular
C_i – soluble intracellular
B_i – bound intracellular

Clearance

k_{tiss}

Soluble C / Bound B — k_{in} / k_{out} — Soluble C_i / Bound B_i

Extracellular   Intracellular

Figure 3.
Modeled processes during the coating dissolution (A) and post coating dissolution (B). Rate-constants: k^T – apparent dissolution rate-constant within the tissue (see text), k_{tiss} – rate-constant of tissue transport, dominated by diffusion (see text); k_{in} and k_{out} are the cell uptake and release time constants. Associated equations and parameter estimates are provided in the online Supplement.
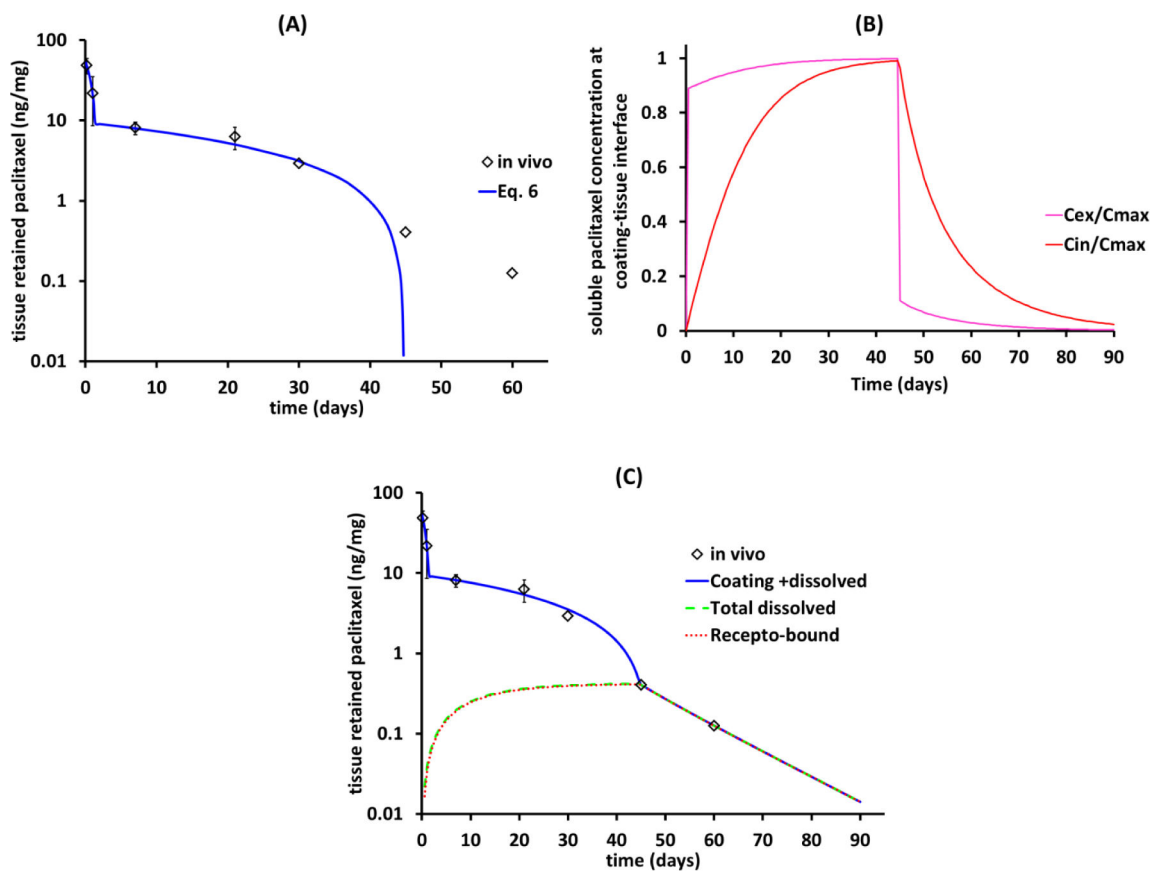
Figure 4.
Resolving *in vivo* tissue retention into solid anhydrous and dissolved paclitaxel for porcine iliofemoral arteries. (A) *In vivo* dissolution of the IN.PACT coating follows piecewise kinetics up to 45d post treatment. (B) Simulated extracellular (C_{ex}) and intracellular (C_{in}) concentrations of soluble paclitaxel at the coating-tissue interface normalized to theoretical $C_{max} = 1.3$ nM (Eq. 7). (C) Simulated bulk tissue concentrations of dissolved paclitaxel, receptor bound (red dashed) and total concentrating of free and bound drug (black line).
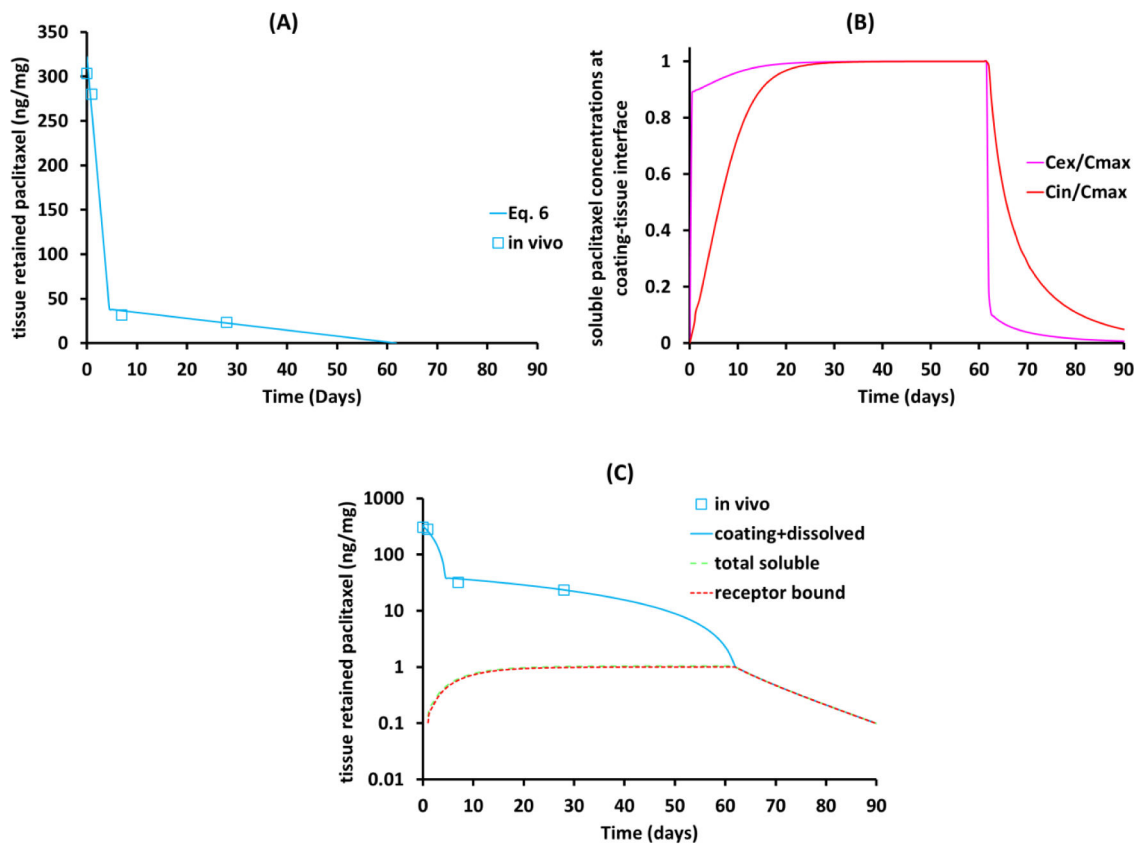
Figure 5.
Resolving *in vivo* tissue retention into solid dihydrate and dissolved paclitaxel for rabbit aorta. (A) *In vivo* dissolution of the dihydrate paclitaxel coating follows beyond 28d and up to 62d post treatment. (B) Simulated extracellular (C_{ex}) and intracellular (C_{in}) concentrations of soluble paclitaxel at the coating-tissue interface normalized to theoretical $C_{max} = 4.3$ nM (Eq. 7). (C) Simulated bulk tissue concentrations of dissolved paclitaxel, receptor bound (red dashed) and total concentrating of free and bound drug (black line).
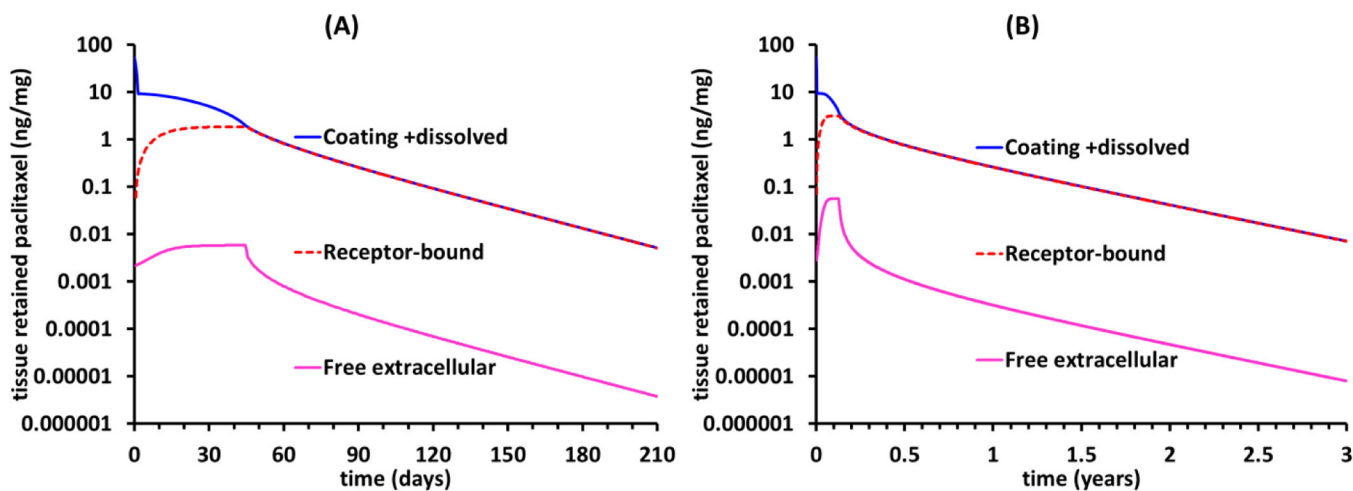
Figure 6.
Hindered diffusion in atherosclerotic arteries prolongs drug retention. Simulations for anhydrous paclitaxel coating assuming a 10-fold (A) or 100-fold (B) diffusive hindrance relative to the cased depicted in Figure 4.

Table 1

Coating retention and tissue dosing parameters in healthy animal arteries as estimated by segmental linear regression(Eq. 6, R^2 0.99)

PCB	Lumenal coating		Tissue coating		
	S_0^L (ng/mg)	T^L (days)	S_0^T (ng/mg)	T^T (days)	$C_{max,sus}$ (nM)
Amorphous[a]	243.8	1.0	0.3	43.7	0.04
Dihydrate[a]	283.9	4.5	38.2	61.9	4.34
IN.PACT™ (anhydrous)[b]	44.4	1.4	9.6	46.7	1.32
Lutonix® [b]	61.	1.1	0.8	221.0	0.02
Ranger™ [b]	49.4	1.4	6.1	41.7	0.94

[a]PCB implanted into rabbit aorta[38].

[b]PCB implanted into porcine iliofemoral[16, 22].

Table 2

Dissolution rate constants of paclitaxel coatings based on their crystallinity.

Paclitaxel form	Aqueous solubility (μg/ml or μM)	Lumenal dissolution rate constants, k^L (d^{-1})	Tissue dissolution rate constants, k^T (d^{-1})
Amorphous	30 μg/ml (35μM) [a]	315.7	3.3[d]
Anhydrous crystal	3.5 μg/ml (3.5 μM) [b]	10.5	0.069
Dihydrate crystal	0.75 μg/ml (0.88 μM) [c]	52.1	0.593

[a] Based on [7, 40].

[b] Based on [6], though published values range up to 6 μg/ml[41].

[c] Average of published values for Dihydrate paclitaxel, 0.36–1.0 μg/ml [6, 7].

[d] Estimated from the lumenal dissolution rate constant, assuming the same lumenal to tissue scaling as for dihydrate paclitaxel.